https://doi.org/10.5194/egusphere-2026-790
Preprint. Discussion started: 30 March 2026

Spatial variability of ^{10}Be in deep ice and the influence of the measurement procedure

Niklas Kappelt[1], Piers Larkman[2], Pascal Bohleber[2, 3], Florian Adolphi[2, 4], Marcus Christl[5], Christof Vockenhuber[5], Philip Gautschi[5], Eric Wolff[6], and Raimund Muscheler[1]

[1]Department of Geology, Lund University, Sölvegatan 12, 22362 Lund, Sweden
[2]Alfred Wegener Institute Helmholtz Centre for Polar and Marine Research, Am Handelshafen 5, 27570 Bremerhaven, Germany
[3]Goethe University Frankfurt am Main, Altenhöferallee 1, 60438 Frankfurt am Main, Germany
[4]Faculty of Geosciences, University of Bremen, Klagenfurter Str. 2-4, 28359 Bremen, Germany
[5]Laboratory of Ion Beam Physics, Swiss Federal Institute of Technology, Otto-Stern Weg 5, 8093 Zürich, Switzerland
[6]Department of Earth Sciences, University of Cambridge, Downing Street, CB2 3EQ Cambridge, United Kingdom

Correspondence: Raimund Muscheler (raimund.muscheler@geol.lu.se)

Abstract. Concentrations of the radionuclide ^{10}Be are often measured in ice cores to reconstruct solar activity and the geomagnetic field, as well as to improve, verify and extend timescales. However, concentration spikes in deep ice, concentrations decreasing faster with age than possible through radioactive decay, and an increasing dust association with depth suggest ^{10}Be is subject to post-depositional processes, which can alter measured ^{10}Be concentrations, that are poorly understood.

In ice from EPICA Dome C, we analysed the progression of horizontal ^{10}Be variability with depth, the effect of ion exchange columns and acidic treatment on the measured concentrations, and the potential influence of the microstructure. We found that acidic treatment had no effect on the measurement results, while samples treated through ion exchange columns showed a reduction in measured ^{10}Be concentrations of up to 40 %, with the proportion apparently increasing with depth and age. This is the likely cause for the apparent loss of ^{10}Be in deep ice in a previous study. We found that even in samples as small as ($10 \times 1.5 \times 1.5$) cm^3 (ca. 20 g), the grain boundary content does not vary significantly between samples, while ^{10}Be concentrations differ, so ^{10}Be cannot be homogenously distributed along grain boundaries. However, our data suggests an increase of the horizontal variability with depth, in agreement with a possible local accumulation and depletion of ^{10}Be over time.

1 Introduction

The concentrations of the radionuclide ^{10}Be in ice cores are of interest for several reasons. It has a half-life of 1.387 Myr (Chmeleff et al., 2010) and is atmospherically produced in spallation reactions induced by galactic cosmic rays. It's production rate depends on the solar magnetic and geomagnetic field strengths, as both fields modulate the galactic cosmic ray flux reaching Earth. Therefore, ^{10}Be concentrations in ice cores are used in reconstructions of both the solar magnetic field (Nguyen et al., 2022; Nilsson et al., 2024), and the geomagnetic field (Muscheler et al., 2005; Zheng et al., 2021). ^{10}Be concentrations are also used as time markers as peaks in the production rate, caused by e.g. geomagnetic field reversals or solar storms, are often recorded in different archives whose chronologies can be aligned (Adolphi and Muscheler, 2016; Raisbeck et al., 2006;

https://doi.org/10.5194/egusphere-2026-790
Preprint. Discussion started: 30 March 2026

Mulvaney et al., 2023). Together with ^{36}Cl, the ^{36}Cl/^{10}Be ratio can also provide absolute age estimates, as ^{36}Cl decays with a half-life of 301 kyr (Endt and van dèr Leun, 1973) and the ratio theoretically minimises the influences of variable radionuclide production, transport and deposition since these processes affect both radionuclides similarly (Kappelt et al., 2025a; Wagner et al., 2000). It has been used to estimate the age of basal ice in the Dye-3 and Greenland Ice Core Project (GRIP) ice cores in Greenland and the Skytrain ice core in West Antarctica (Kappelt et al., 2025a, b; Willerslev et al., 2007). However, the ^{10}Be concentration in the EPICA Dome C (EDC) ice core was found to decrease faster than one would expect from physical decay alone, potentially leading to an underestimation of the age, when using the ^{36}Cl/^{10}Be ratio (Kappelt et al., 2025a). Similarly, older age estimates were obtained with ^{36}Cl alone than with the ratio at Skytrain, hinting towards low measured ^{10}Be concentrations in the bottommost ice.

The post-depositional behaviour of ^{10}Be is poorly understood, making the resulting uncertainty difficult to estimate. For the GRIP ice core, it has been shown that the fraction of dust-associated ^{10}Be increases with depth (Baumgartner et al., 1997; Wagner, 1998), confirming a post-depositional change, which can have a depth-dependent effect on the measured concentration if dust is removed through sample filtration. Further evidence for post-depositional alteration stems from the EPICA Dronning Maud Land (EDML) ice core, in which a ten-fold increase of the ^{10}Be concentration was detected in a sample about 20 m above bedrock, too large for a production- or deposition-related effect (Auer et al., 2009). Instead, acidic liquid phases at grain boundaries and triple junctions may enable the mobility of ^{10}Be and other impurities (de Angelis et al., 2013; Fukazawa et al., 1998; Sakurai et al., 2017; Mulvaney et al., 1988). Localised concentration spikes were also found by Raisbeck et al. (2006) in the EDC core. They imply a depletion elsewhere, potentially compromising the purpose of a production signal correction of ^{36}Cl with ^{10}Be, depending on the diffusion length and the sample size.

Additionally, it has been shown that the acidic brines at grain boundaries promote geochemical reactions and remineralisation (Baccolo et al., 2021), potentially leading to the formation of new beryllium compounds or the inclusion of beryllium in compounds, which may prevent the quantitative detection of ^{10}Be. In this case, variations of the preparation methods used in different studies and by different research groups could lead to different results. For example, the degree of ^{10}Be leaching or particle dissolution can occur depending on different factors: the type of acid (hydrochloric acid (HCl) or nitric acid (HNO_3)) contained in the ^{9}Be carrier solution that is added to the sample, the resulting pH, and the elapsed time. In some studies, beryllium is precipitated directly from the meltwater (Raisbeck et al., 2006; Nguyen et al., 2021), but the standard approach is an isolation from the meltwater with ion exchange columns (IEC) with subsequent acidic elution (e.g., Adolphi et al., 2014; Raisbeck et al., 1981). Comparisons of the approaches, however, are sparse.

In this study, we analysed the variability of ^{10}Be concentrations among replicates at a given depth in discrete EDC ice core samples with ages between 22 and 738 kyr BP. Additionally, different sample preparation procedures involving acidic treatments and the use of ion exchange columns were tested in aliquots of a given sample to compare their potential influence on the measured ^{10}Be concentration. Complementary to this radionuclide bulk analysis, variability in the microstructure of selected samples was compared to measured ^{10}Be concentrations, allowing for a discussion of the influence of geometric differences between adjacent samples.

https://doi.org/10.5194/egusphere-2026-790
Preprint. Discussion started: 30 March 2026

2 Methods

2.1 Ice samples

The Antarctic Ice Core Chronology 2023 (AICC23) extends to an age of 813 kyr BP at a depth of 3193 m in the EDC core. In our study, we analysed one EDC sample approximately every 100 kyr, using a total of eight A-cuts (Fig. S1), each representing roughly a quarter section of a 10 cm diameter core, 55 cm in length. Specific samples were selected based on non-sea-salt calcium concentrations above 20 µg kg^{-1} and a Cl^-/Na^+close to the sea-salt reference value of 1.80, as ^{36}Cl loss is limited or absent in these samples, making them most relevant for the application of the ^{36}Cl/^{10}Be ratio as a dating method (Röthlisberger et al., 2003; Kappelt et al., 2025a). The A-cuts were processed according to the cutting scheme illustrated in Figure S1, dividing each of them into five lengths of about 10 cm with seven replicates from each depth. The A-cuts from bags 5302 and 5708 were shorter than 55 cm and accordingly divided into only four and three lengths, respectively. Individual sample weights ranged from approximately 20–40 g.

A second set of samples was obtained from the Skytrain ice core in West Antarctica, which is 651 m deep and 126 kyr old, 24 m above bedrock with much older ice at the base (Mulvaney et al., 2023; Kappelt et al., 2025b). In a previous study (Kappelt et al., 2025b), we measured the ^{36}Cl/^{10}Be ratio in 18 samples weighing about 1.3 kg. From ten of these samples, about 80 g of ice was removed from the side to obtain a second ^{10}Be measurement representative of the same depth to allow us to assess the variability within the ice core.

2.2 Large area scanning microscopy

The microstructure of EDC samples from eight different depth sections was analysed. Three replicate samples with an approximate geometry of 9.5 by 1.5 by 1.5 cm from each depth sections were microtomed and left to sublimate for about two hours to create a smooth surface, which was subsequently scanned with a large area scanning microscope, which has been described by Kipfstuhl et al. (2006). This process returns an image where grain boundaries and other inclusions in the ice appear dark, against a light colour of grain interiors.

To return a simple segmentation, approximately parametrising the microstructural geometry of the samples a simplified approach referencing an existing LASM image processing procedure (Binder et al., 2013) was developed. The images were processed using CellPose SAM, an image segmentation tool (Stringer et al., 2021), to identify each grain-region in an image. The average region size and the ratio of grain boundary to grain interior pixels was subsequently extracted from the processed image. Dark regions were excluded from the analysis; these correspond to bubbles and damaged regions of the samples.

2.3 Radionuclide measurements

Following the non-destructive LASM analysis, all EDC samples were prepared for ^{10}Be measurements by weighing them and adding 0.15 mg of ^{9}Be carrier (0.15 mL of ICP standard with 1 mg/mL and 3 % HNO_3) to each of the frozen samples, which were left to melt at room temperature in 50 mL centrifuge tubes (see schematic in Figure 1).

https://doi.org/10.5194/egusphere-2026-790
Preprint. Discussion started: 30 March 2026

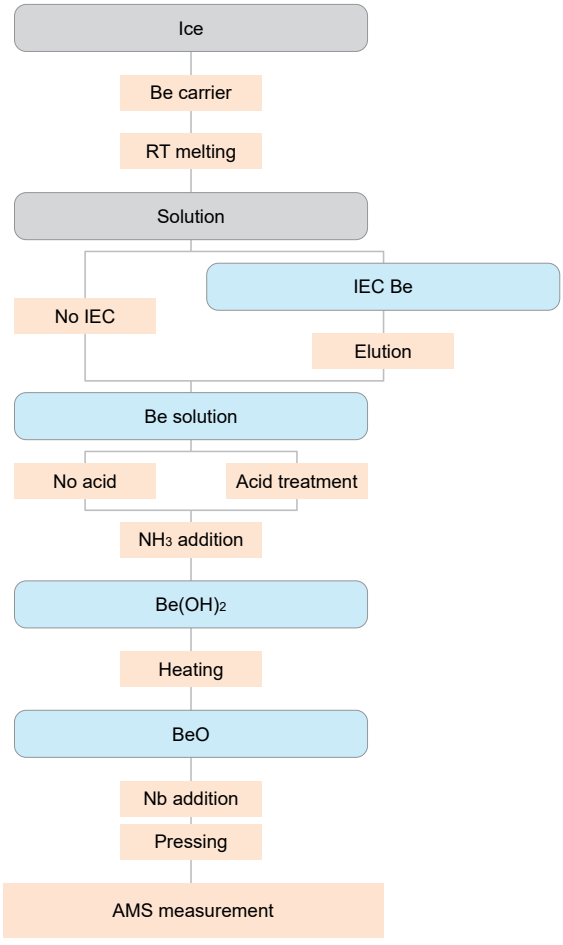

Figure 1. Overview of the ^{10}Be sample preparation with optional acidic treatment and use of ion exchange columns. RT: Room Temperature, IEC: Ion Exchange Column, AMS: Accelerator Mass Spectrometer.

https://doi.org/10.5194/egusphere-2026-790
Preprint. Discussion started: 30 March 2026

2.3.1 Precision samples

To define the reproducibility of ^{10}Be measurements, EDC samples from five different depth sections were analysed. From each section, four replicate samples were first homogenised and then split into four aliquots. Two aliquots received 2 mL 65 $\%$ $\mathrm{HNO_3}$, resulting in a pH of 0–0.5, and two aliquots received no acidic treatment, resulting in a pH of 2–3. Beryllium was directly precipitated in all samples.

2.3.2 Ion exchange column samples

In a test series to assess the influence of ion exchange column extraction in comparison to direct precipitation, EDC samples from seven different depth sections were analysed. From each section, four replicates were homogenised and split into four aliquots. Two aliquots were run through ion exchange columns, which were subsequently eluted with about 25 mL 4 $\mathrm{M\ HCl}$. In the other two aliquots, beryllium was directly precipitated. The two approaches represent the standard extraction with and without ion exchange columns.

2.3.3 Acidic treatment samples

In a second series of experiments, we tested whether different acidic treatments lead to different degrees of leaching and particle dissolution and therefore have an effect on measured ^{10}Be concentrations. To determine whether the sample's depth and age are relevant to the effect, EDC samples from seven different depth sections were analysed. From each section, three replicate samples were homogenised in a beaker and split into three alqiuots. One aliquot was treated with 2 mL 65 $\%$ $\mathrm{HNO_3}$, one aliquot with 2 mL 65 $\%$ $\mathrm{HNO_3}$ and 0.6 mL 40 $\%$ HF, and one aliquot received no acidic treatment. All solutions were left to react for five days, after which HF samples were heated and reduced to a few mL to evaporate HF. This process was repeated after the addition of 1 mL 65 $\%$ $\mathrm{HNO_3}$. Beryllium was afterwards directly precipitated in all of these samples.

2.3.4 Horizontal variability samples

A third series of experiments was aimed at defining the horizontal ^{10}Be variability within the EDC ice core at seven different depths and comparing the ^{10}Be concentrations to the results of the microstructure analysis. From each depth section, seven replicate samples, including the LASM samples, were treated with 2 mL 65 $\%$ $\mathrm{HNO_3}$. Then beryllium was directly precipitated.

The ten additional Skytrain ice core samples were melted in plastic containers with 150 mg of added ^{9}Be carrier (ICP standard with 3 $\%$ $\mathrm{HNO_3}$) and run through ion exchange columns, which were eluted with about 25 mL 4 $\mathrm{M\ HCl}$.

2.3.5 Measurement procedure

Regardless of whether ion exchange columns were used, acids were added or no special treatment was applied, the pH of all samples was increased to at least 9 by the addition of the necessary volume of 25 $\%$ ammonia ($\mathrm{NH_3}$) to precipitate beryllium hydroxide ($\mathrm{Be(OH)_2}$) overnight. Then, the samples were centrifuged to accumulate $\mathrm{Be(OH)_2}$ at the bottom of their container and the solution was decanted. This process was repeated after adding 8 mL of Milli-Q water for washing. The remaining

https://doi.org/10.5194/egusphere-2026-790
Preprint. Discussion started: 30 March 2026

$Be(OH)_2$ was transferred to a quartz glass crucible, which was heated for about two hours to evaporate all water and then placed into an oven, where it was oxidised to beryllium oxide (BeO) at a temperature of 850 °C overnight. Together with 1 mg of niobium, the beryllium oxide was then transferred to a target and pressed into a small tablet.

The $^{10}Be/^{9}Be$ ratio was measured using Accelerator Mass Spectrometry (AMS) at the Laboratory for Ion Beam Physics, ETH Zurich. $^{10}Be/^{9}Be$ ratios were normalised to the in-house standard S2007N, which has a nominal ratio of $^{10}Be/^{9}Be = (28.1 \pm 0.8) \cdot 10^{-12}$. This standard is, in turn, calibrated against the ICN 01-5-1 standard with a nominal value of $^{10}Be/^{9}Be = 2.709 \cdot 10^{-11}$ (Nishiizumi et al., 2007; Christl et al., 2013). All ^{10}Be samples were corrected with blanks that were prepared in parallel to the corresponding samples.

3 Results and Discussion

3.1 Measurement precision

To determine the precision of repeat measurements, the ^{10}Be concentration was measured in two aliquots of homogenised sub-samples from different depths, both without acidic treatment and directly precipitated. Figure 2 demonstrates the good reproducibility between aliquots and the precision of 2517 $\mathrm{at\,g^{-1}}$, taken as the one-σ standard deviation of the differences shown in panel B. This is similar to the standard deviation among blank samples prepared without acidic treatment and IECs (2442 $\mathrm{at\,g^{-1}}$ in a 25 g sample), so the blank correction appears to determine the precision. In analogous repeat measurements of five pairs of aliquots treated with nitric acid, the precision was slightly worse with 6609 $\mathrm{at\,g^{-1}}$, while nitric acid treated blanks without IECs had a lower standard deviation of 560 $\mathrm{at\,g^{-1}}$ in a 25 g sample (see Figure S3 in the supplement).

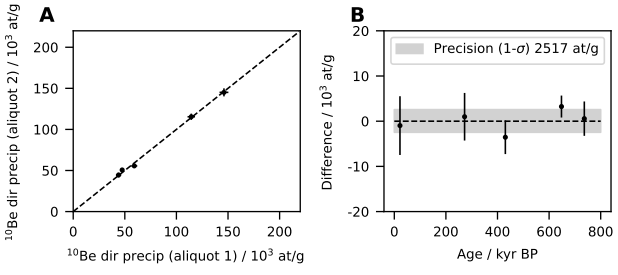

Figure 2. A ^{10}Be concentrations after direct precipitation of berylliumin two aliquots of samples from different depths at EDC. The identity line, where y = x, is shown as a dashed line. **B** The differences between the two aliquots and their one-σ standard deviation from the mean. Errorbars in the two panels indicate one-σ measurement uncertainties and the uncertainties resulting from Gaussian error propagation, respectively.

https://doi.org/10.5194/egusphere-2026-790
Preprint. Discussion started: 30 March 2026

3.2 Influence of ion exchange columns

After the addition of ^{9}Be carrier, ice core samples are usually melted and passed through ion exchange columns to isolate Be, as this reduces the sample size, acts as a pre-concentration step and simplifies the aqueous chemistry (Raisbeck and Yiou, 1985; Nguyen et al., 2021). As AMS systems became more capable, the required sample mass decreased to less than 50 g, samples were able to fit into regular centrifuge tubes and ^{10}Be could be precipitated directly. To assess whether the choice of preparation method has an effect on the resulting ^{10}Be concentration, we split samples from different depths into two and precipitated beryllium directly in one aliquot while running the other through an ion exchange column with subsequent elution using 4 $\mathrm{M\ HCl}$. As shown in Figure 3, lower ^{10}Be concentrations were measured in the IEC treated aliquot of all samples. While the absolute difference only increases from about 10,000 $\mathrm{at\,g^{-1}}$ in shallower samples to 20,000 $\mathrm{at\,g^{-1}}$ in deeper samples, as shown in panel (B), the deficit relative to the directly precipitated aliquot increases to about 40 $\%$ (panel (C)), due to overall lower ^{10}Be concentrations in the older ice. The largest absolute difference is observed for the sample with the highest ^{10}Be concentration and an age of about 150 kyr. More data is needed to understand whether this is an outlier or a replicable effect in samples with high ^{10}Be concentrations. The uncertainty of the ^{10}Be concentration in the 150 kyr old sample is comparatively large, but the high current measured for ^{9}Be in the AMS provides no reason to doubt the value.

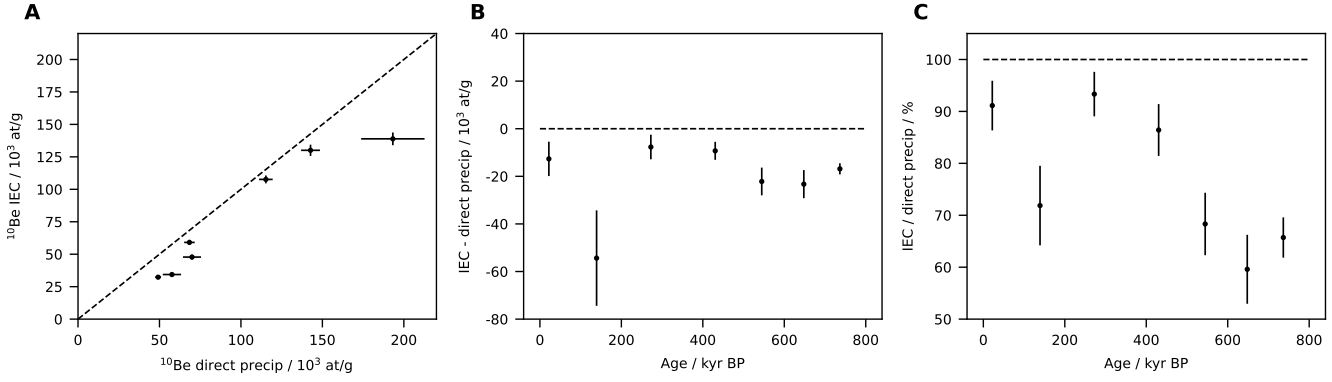

Figure 3. A ^{10}Be concentrations after isolation with IECs compared to direct precipitation of beryllium in two aliquots of samples from different depths at EDC. The identity line, where y = x, is shown as a dashed line. Errorbars indicate one-σ measurement uncertainties. **B** The absolute differences between the two aliquots. Errorbars indicate the uncertainties resulting from Gaussian error propagation of the measurement uncertainties in the first panel. **C** The ^{10}Be concentration after IEC isolation relative to direct precipitation. Errorbars indicate the uncertainties resulting from Gaussian error propagation of the measurement uncertainties in the first panel.

In a study of ^{10}Be in drill chips from Little Dome C, Nguyen et al. (2021) also tested whether direct precipitation would produce different results compared to the procedure using ion exchange columns and found that there was no significant difference in surface drill chips as well as in fresh snow samples from Lund in Sweden. In our results, the reduction in two out of three samples younger than 400 kyr is not significant at the 95 $\%$ confidence level, suggesting that the effect can be negligible in some samples near the surface and thus not contradicting the findings of Nguyen et al. (2021). A possible explanation for

https://doi.org/10.5194/egusphere-2026-790
Preprint. Discussion started: 30 March 2026

the decreasing IEC ^{10}Be concentrations with depth could be the an increasing association of ^{10}Be with dust, which has been observed in the GRIP ice core in Greenland (Baumgartner et al., 1997; Wagner, 1998). IECs may act as a filter for dust particles and the standard leaching procedure may be insufficient to recover all ^{10}Be. Alternatively, dust particles (containing ^{10}Be) may not be retained in the column during the deposition stage, when beryllium is supposed to bind to the resin, and are therefore lost before the elution stage, when beryllium is supposed to be released again. The observed decrease is also of the same magnitude as the apparently missing ^{10}Be in our earlier radionuclide study at EDC, where an exponential fit of the ^{10}Be flux versus age yielded a half-life of 618 $\pm$ 78 kyr, far smaller than the actual half-life of 1387 kyr (Kappelt et al., 2025a). Panel (C) of Figure 3 roughly suggests a loss of 5 % at present day, which increases to about 40 % at 800 kyr BP. If a corresponding correction is applied to previously published data Kappelt et al. (2025a), an exponential fit yields a half-life of 1226 $\pm$ 302 kyr, close to the actual half-life. The dust associated fraction of ^{10}Be in the GRIP ice core increases similarly to the percentage lost in IECs from about 10 % at the surface to 50 % at about 3000 m depth (Baumgartner et al., 1997; Wagner, 1998).

3.3 Acidic treatment

To test the influence of acidic treatment, homogenised sub-samples from different depths were split into two aliquots, one left untreated and one treated with nitric acid, as described in Section 2.3. beryllium was then precipitated directly in both aliquots. The standard deviation of differences between HNO_3 treated and untreated ^{10}Be concentrations is 14,240 at g^{-1}, as shown in Figure 4. Contrary to the comparison of IEC treated and directly precipitated samples, the treatment with HNO_3 either lead to an increase or decrease of the measured ^{10}Be concentration; the mean difference between treated and untreated samples is -116 at g^{-1}, close to zero. The largest outlier is found in a sample with an age of about 150 kyr, which is referenced against the high ^{10}Be concentration of a directly precipitated sample already mentioned in the discussion of Figure 3.

It is unclear what causes the deviation in both directions and the larger variability of differences. Our hypothesis was to detect higher ^{10}Be concentrations in samples treated with HNO_3, as potential newly formed ^{10}Be containing compounds in deep ice would be dissolved. A contribution of stable ^{9}Be through dissolution of continental dust would theoretically lead to a decrease, but dust concentrations are low in the EDC core and the natural beryllium content in dust is low. With a crustal Be/Ca fraction of 6.2 $\cdot 10^{-5}$ (Wedepohl, 1995) and a maximum nss-Ca^{2+} concentration of 80 ppb, the natural beryllium content is about 1 million times smaller than the added ^{9}Be carrier in a 30 g sample, even in a kilogram of ice the contribution is negligible. A possible contamination of either ^{10}Be or ^{9}Be from nitric acid can also be excluded, as the ^{10}Be/^{9}Be ratios measured in blanks with nitric acid addition ($(7.7 \pm 1.0) \cdot 10^{-15}$) and in blanks without it ($(9.3 \pm 1.2) \cdot 10^{-15}$) were identical within the uncertainty.

Our data suggests that there are no acid-soluble ^{10}Be-containing compounds which are left undetected without an acidic treatment of the sample, as the mean concentration difference between HNO_3 treated and untreated samples is close to zero.

One of two possible explanations would be that newly formed ^{10}Be-containing compounds are already dissolved and ^{10}Be adsorbed to dust is already leached effectively without the addition of HNO_3, due to the acidification to pH 2–3 from the carrier solution. However, the discrepancy between IEC treated and directly precipitated samples presented in the previous section would remain unexplained in this case. Alternatively, new ^{10}Be-containing compounds are formed or ^{10}Be attach strongly to particles and a lower pH has no influence on the degree of dissolution or leaching, but the compounds or particles

https://doi.org/10.5194/egusphere-2026-790
Preprint. Discussion started: 30 March 2026

are precipitated alongside $Be(OH)_2$ and effectively ionised in the AMS with quantitative detection of ^{10}Be, while IECs remove them, leading to higher ^{10}Be concentrations in directly precipitated samples.

Only in two out of seven samples treated with HF in addition to HNO_3, could beryllium be measured. An incomplete evaporation of HF may have prevented the precipitation of $Be(OH)_2$ in the other five samples, but as acidic treatment did not appear useful in the sample preparation procedure the experiments were not repeated.

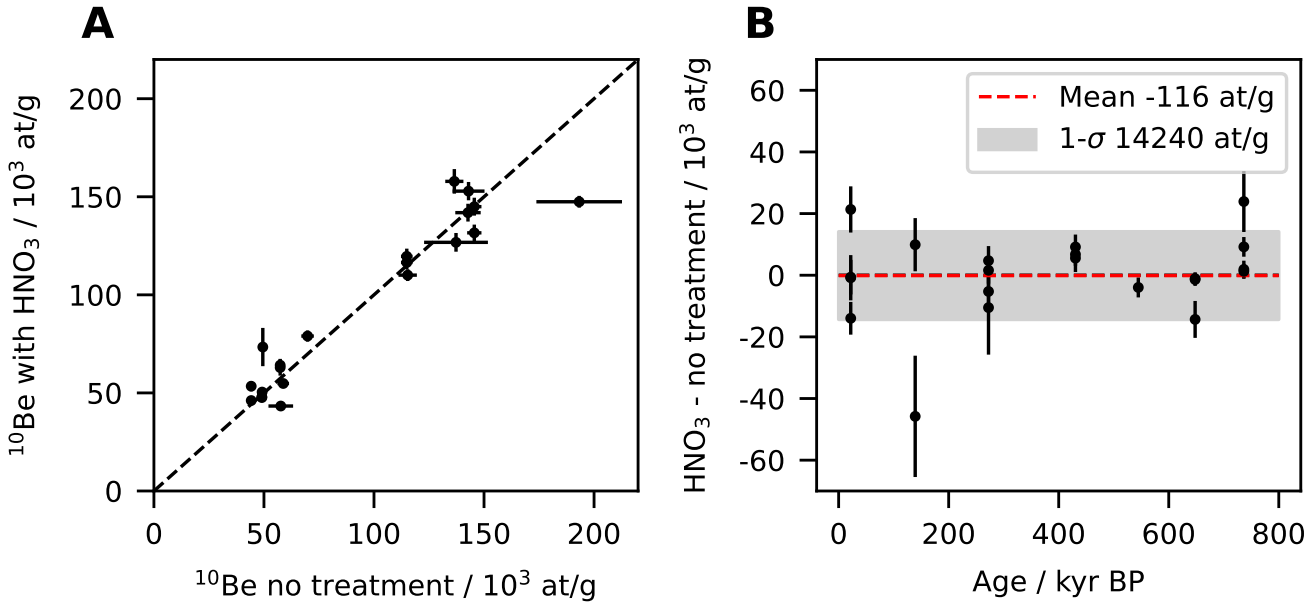

Figure 4. A Comparison of measured ^{10}Be concentrations in aliquots without acidic treatments and ^{10}Be concentrations measured in aliquots with nitric acid treatment. **B** Absolute concentration differences between aliquots. Errorbars in the two panels indicate one-σ measurement uncertainties and the uncertainties resulting from Gaussian error propagation, respectively.

3.4 Horizontal variability

To assess the horizontal variability of ^{10}Be concentrations in the EDC core, five to seven samples with identical depth ranges were analysed at nine different depths. As they were prepared before the results from the comparison of different preparation methodologies were available, and a positive effect from nitric acid treatment was expected, all of them were acidified and directly precipitated. No spikes similar to those reported by Raisbeck et al. (2006) were found in our samples. While Raisbeck et al. (2006) gave no definition of a spike, one could define them as ^{10}Be concentrations at least 50 % higher than a 5-point running mean, which would classify 49 out of 830 data-points as spikes in their samples. Assuming independent sampling and a constant probability of $p = 49/830 = 0.059$ for finding a peak across datasets, it not unlikely that no peaks were found in the 22 samples with an age older than 600 kyr BP we measured individually, since $P(0) = (1 - 0.059)^{22} = 26$ %. Apart from

https://doi.org/10.5194/egusphere-2026-790
Preprint. Discussion started: 30 March 2026

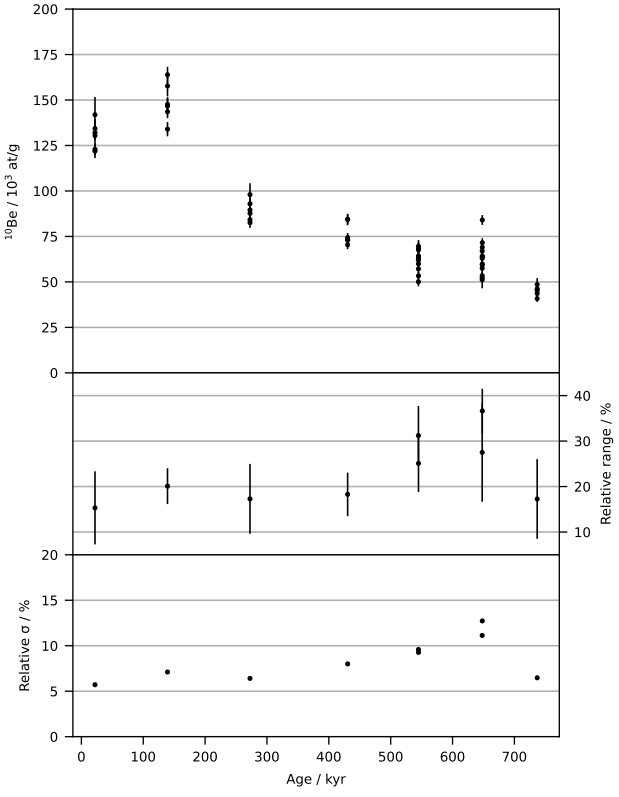

Figure 5. Variability of the ^{10}Be concentration among horizontal replicates from EDC ice of different ages. Replicates from two distinct depths were analysed in in samples from 550 and 650 kyr BP, so there are two values for the range and the standard deviation, respectively, relative to the mean. Errorbars indicate one-σ measurement uncertainties in the first panel and the uncertainties resulting from Gaussian error propagation in the second panel.

https://doi.org/10.5194/egusphere-2026-790
Preprint. Discussion started: 30 March 2026

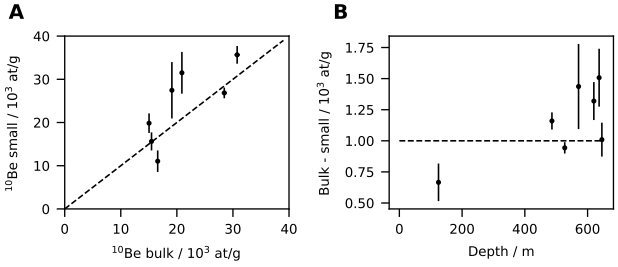

Figure 6. Comparison of ^{10}Be concentration in small replicate samples compared to ^{10}Be concentrations measured in large samples from the Skytrain ice core. Errorbars indicate one-σ measurement uncertainties in the first panel and the uncertainties resulting from Gaussian error propagation in the second panel.

the about 750 kyr old samples, where the absolute range between horizontal replicates was smaller than the detection limit, the data hints at a slight increase of the range and standard deviation among horizontal replicates with higher values around 550 and 650 kyr, as shown in Figure 5, but with the increased variability of ^{10}Be concentrations in HNO_3 treated samples (see Figure S3) the effect is marginal. Raisbeck et al. (2006) suggested that a migration of ^{10}Be occurs predominantly horizontally rather than from adjacent depths, as they found ^{10}Be concentration spikes in the EDC ice core, which could not be removed by smoothing the data over several thousands of years (Raisbeck et al., 2006). Although we saw no extreme enhancements like those seen by Raisbeck et al. (2006) or Auer et al. (2009), our results do suggest that local horizontal variability is occurring, and therefore might be partially responsible for the high variability observed in previous studies.

From several large radionuclide samples (about 1.3 kg) of the Skytrain ice core, thin strips were cut off at the side to compare the ^{10}Be concentration in small (40–80 g) samples from the same depth interval. The large differences between bulk and small samples shown in Figure 6 point in the same direction as the EDC data: there is a significant horizontal variability of ^{10}Be concentrations. The Skytrain and EDC data show that the horizontal variability is of the same magnitude, if not larger, as the vertical signal. The ^{10}Be concentrations measured in two horizontal replicates can be further apart than the ^{10}Be concentrations in two samples of different depths, while not representing any change in the production signal.

3.5 Impurity localisation

A possible explanation for horizontal variability is that some ice within a particular temporal layer may preferentially contain ^{10}Be compared to other ice of the same age. A possible indicator for such preferential redistribution would be the volume density of grain boundaries, assuming co-localisation of ^{10}Be with soluble impurities. Optical and chemical analyses on ice samples have indicated preferential distribution of some chemical species at grain boundaries (Svensson et al., 2011; Bohleber et al., 2024), including measurements collected at variable depths in the EDC ice core (Larkman et al., 2025), suggesting that variability in impurity measurements could arise due to changes in grain geometry (Ng, 2021). Assuming an accumulation at grain boundaries, the ^{10}Be content of a sample could depend on the total grain boundary length. In rather shallow ice (EDC 951, depth 523 m), where grains are small compared to the sample size, little variability was expected for the grain boundary content

https://doi.org/10.5194/egusphere-2026-790
Preprint. Discussion started: 30 March 2026

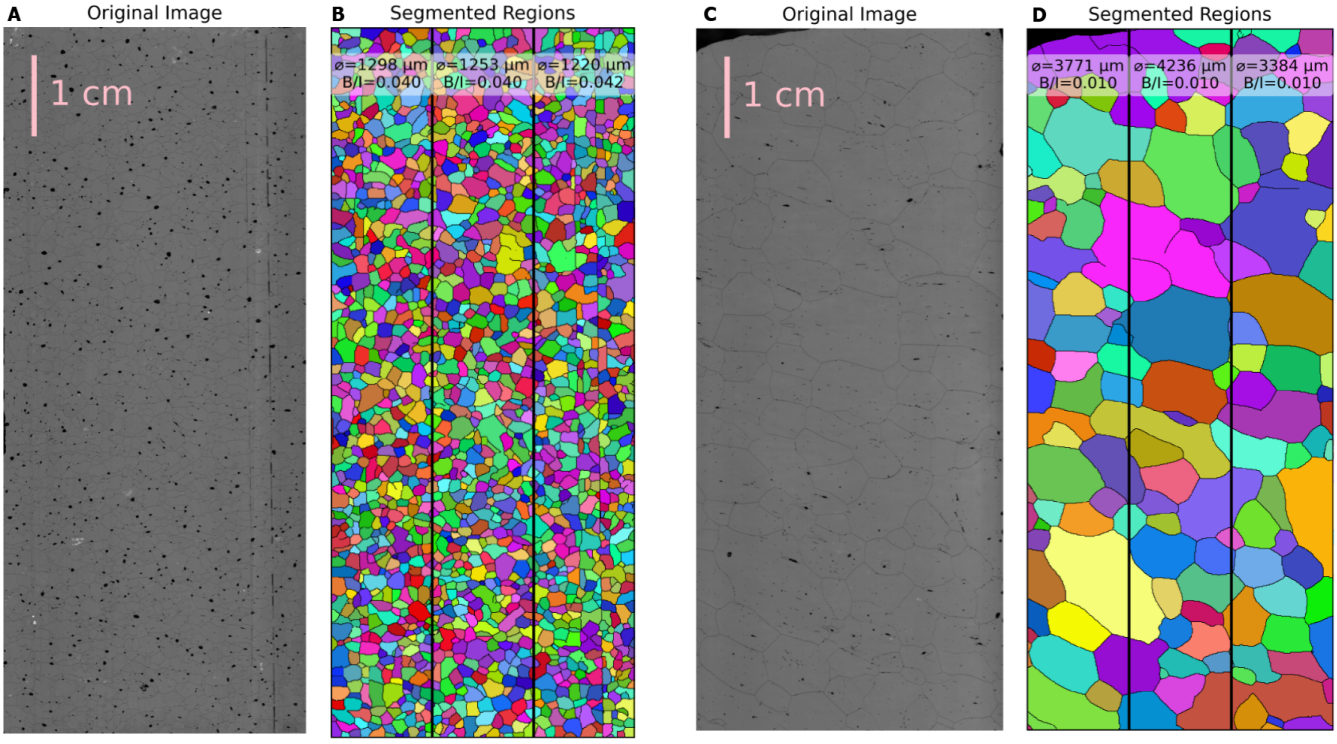

Figure 7. LASM data (**A** and **C**) and resulting region segmentations (**B** and **D**) from the EDC 951 (**A** and **B**, depth 523 m, age 22 kyr) and EDC 5540 (**C** and **D**, depth 3046 m, age 648 kyr) samples. The scale bar corresponds to both images for each sample. The ⌀ value indicates the effective mean region diameter and B/I the boundary to interior ratio for each of the three horizontally separated sections indicated by black bars in B and D. Similar plots for samples from other depths can be found in the supplementary material.

of horizontal replicates. Figure 7B confirms this with the calculated ratio of grain boundary to grain interior pixels *B/I*, which lies between 0.040 and 0.042 for three replicates with grains of about 1 mm diameter. In deep samples such as EDC 5540, depth 3046 m (Figure 7D), which feature much larger grains of about 4 mm diameter on average, variation in grain size is seen between regions as the average diameter is of the same order as replicate width. However, the boundary to interior ratio does not show meaningful variability between replicates, lying at 0.010. At the same time, the blank corrected ^{10}Be concentrations in samples EDC 5540 B1 (central sample of Figure 7D) and EDC 5540 C1 (right-hand sample of Figure 7D) were $(6.70 \pm 0.41) \cdot 10^4$ at g^{-1} and $(5.12 \pm 0.47) \cdot 10^4$ at g^{-1}, respectively. Assuming that the variability of the calculated grain boundary content is equally low in three dimensions, we conclude that there are no geometric differences to consider and the same length of grain boundaries can be expected in any chosen sample from depths measured in this study. An accumulation on dust particles, which can form localised aggregates (de Angelis et al., 2013) appears more likely and could invoke the observed horizontal variability.

https://doi.org/10.5194/egusphere-2026-790
Preprint. Discussion started: 30 March 2026

4 Conclusions

We found significantly lower ^{10}Be concentrations in samples that were passed through ion exchange columns compared to samples from which ^{10}Be was directly precipitated. The discrepancy increased from about 5 % near the surface to about 40 % at the bottom of the core. This difference is of the same magnitude as the apparently missing ^{10}Be in deep ice from a previous study of radionuclides in the EDC ice core. We, therefore, suggest that the low concentrations were caused by the treatment with ion exchange columns and related to the increasing association of ^{10}Be with dust. Either, dust with attached ^{10}Be was retained in the columns and leaching was insufficient to recover all ^{10}Be or dust containing ^{10}Be was not retained in the first place and flushed out with the meltwater, while only dissolved beryllium remained in the column. In future experiments, this can be tested by leaching IECs with more or stronger acids.

While no ^{10}Be spikes similar to those reported by Raisbeck et al. (2006) were found, a slight increase of the variability of ^{10}Be concentrations among horizontal replicates suggests a possible migration of ^{10}Be resulting in the local accumulation and depletion of ^{10}Be. While an increased association with dust is likely, a homogenous co-location at grain boundaries does not seem plausible, as the fraction of grain boundary to interior was similar among horizontal replicate samples with different ^{10}Be concentrations. The horizontal variability suggests that concentrations of individual samples in ice nearer to the bed should not be over-interpreted (for example suggesting age reversals), but rather smoothing over a number of samples should be used for dating and synchronisation procedures.

We recommend measuring ^{10}Be in deep ice without the use of ion exchange columns if possible and testing whether the ^{10}Be deficit in samples prepared with ion exchange columns can be replicated with ice from other drill sites. Testing should also be carried out to determine whether the recovery of ^{10}Be from IECs can be improved through better leaching.

Data availability. The radionuclide data are available at zenodo.org via https://doi.org/10.5281/zenodo.16810909 with license Creative Commons Attribution 4.0 International.

Author contributions. NK, PL, PB, FA, and RM designed the study; NK, PB, EW, and RM acquired funding; NK, PL, MC, CV, and PG performed the measurements; NK and PL analysed and visualised the data; NK and PL wrote the article; all co-authors reviewed and edited the article.

Competing interests. The contact author has declared that none of the authors has any competing interests.

Acknowledgements. This project has received funding from the European Union's Horizon 2020 research and innovation programme under the Marie Skłodowska-Curie grant agreement No 955750. Pascal Bohleber and Piers Larkman gratefully acknowledge funding by the

https://doi.org/10.5194/egusphere-2026-790
Preprint. Discussion started: 30 March 2026

European Union (ERC, AiCE, 101088125). This work is a contribution to the European Project for Ice Coring in Antarctica (EPICA), a joint European Science Foundation–European Commission (EC) scientific programme funded by the EU and by national contributions from Belgium, Denmark, France, Germany, Italy, the Netherlands, Norway, Sweden, Switzerland and the UK. The main logistic support at Dome C was provided by IPEV and PNRA. This is EPICA publication no. X. The Skytrain ice core was collected through the European Research Council under the Horizon 2020 research and innovation programme (grant agreement no. 742224, WACSWAIN).

https://doi.org/10.5194/egusphere-2026-790
Preprint. Discussion started: 30 March 2026

References

Adolphi, F. and Muscheler, R.: Synchronizing the Greenland ice core and radiocarbon timescales over the Holocene-Bayesian wiggle-matching of cosmogenic radionuclide records, Climate of the Past, 12, 15–30, https://doi.org/10.5194/cp-12-15-2016, 2016.

Adolphi, F., Muscheler, R., Svensson, A., Aldahan, A., Possnert, G., Beer, J., Sjolte, J., Björck, S., Matthes, K., and Thiéblemont, R.: Persistent link between solar activity and Greenland climate during the Last Glacial Maximum, Nature Geoscience, 7, 662–666, https://doi.org/10.1038/ngeo2225, 2014.

Auer, M., Wagenbach, D., Wild, E. M., Wallner, A., Priller, A., Miller, H., Schlosser, C., and Kutschera, W.: Cosmogenic 26Al in the atmosphere and the prospect of a 26Al/10Be chronometer to date old ice, Earth and Planetary Science Letters, 287, 453–462, https://doi.org/10.1016/j.epsl.2009.08.030, 2009.

Baccolo, G., Delmonte, B., Stefano, E. D., Cibin, G., Crotti, I., Frezzotti, M., Hampai, D., Iizuka, Y., Marcelli, A., and Maggi, V.: Deep ice as a geochemical reactor: Insights from iron speciation and mineralogy of dust in the Talos Dome ice core (East Antarctica), Cryosphere, 15, 4807–4822, https://doi.org/10.5194/tc-15-4807-2021, 2021.

Baumgartner, S., Beer, J., Wagner, G., Kubik, P., Suter, M., Raisbeck, G., and Yiou, F.: 10Be and dust, Nuclear Instruments and Methods in Physics Research Section B: Beam Interactions with Materials and Atoms, 123, 296–301, https://doi.org/10.1016/S0168-583X(96)00751-3, 1997.

Binder, T., Garbe, C. S., Wagenbach, D., Freitag, J., and Kipfstuhl, S.: Extraction and parametrization of grain boundary networks in glacier ice, using a dedicated method of automatic image analysis, J. Microsc., 250, 130–141, 2013.

Bohleber, P., Larkman, P., Stoll, N., Clases, D., de Vega, R. G., Šala, M., Roman, M., and Barbante, C.: Quantitative Insights on Impurities in Ice Cores at the Micro-Scale From Calibrated LA-ICP-MS Imaging, Geochemistry, Geophysics, Geosystems, 25, https://doi.org/10.1029/2023GC011425, 2024.

Chmeleff, J., von Blanckenburg, F., Kossert, K., and Jakob, D.: Determination of the 10Be half-life by multicollector ICP-MS and liquid scintillation counting, Nuclear Instruments and Methods in Physics Research Section B: Beam Interactions with Materials and Atoms, 268, 192–199, https://doi.org/10.1016/j.nimb.2009.09.012, 2010.

Christl, M., Vockenhuber, C., Kubik, P. W., Wacker, L., Lachner, J., Alfimov, V., and Synal, H.-A. A.: The ETH Zurich AMS facilities: Performance parameters and reference materials, Nuclear Instruments and Methods in Physics Research, Section B: Beam Interactions with Materials and Atoms, 294, 29–38, https://doi.org/10.1016/j.nimb.2012.03.004, 2013.

de Angelis, M., Tison, J. L., Morel-Fourcade, M. C., and Susini, J.: Micro-investigation of EPICA Dome C bottom ice: Evidence of long term in situ processes involving acid-salt interactions, mineral dust, and organic matter, Quaternary Science Reviews, 78, 248–265, https://doi.org/10.1016/j.quascirev.2013.08.012, 2013.

Endt, P. and van dèr Leun, C.: Energy levels of A = 21-44 nuclei (V), Nuclear Physics A, 214, 1–625, https://doi.org/10.1016/0375-9474(73)91131-7, 1973.

Fukazawa, H., Sugiyama, K., Mae, S., Narita, H., and Hondoh, T.: Acid ions at triple junction of Antarctic ice observed by Raman scattering, Geophysical Research Letters, 25, 2845–2848, https://doi.org/10.1029/98GL02178, 1998.

Kappelt, N., Muscheler, R., Baroni, M., Beer, J., Christl, M., Vockenhuber, C., Bard, E., and Wolff, E.: Ice core dating with the 36Cl/10Be ratio, Quaternary Science Reviews, 355, 109 254, https://doi.org/10.1016/j.quascirev.2025.109254, 2025a.

Kappelt, N., Wolff, E., Christl, M., Vockenhuber, C., Gautschi, P., and Muscheler, R.: 500-thousand-year-old basal ice at Skytrain Ice Rise, West Antarctica, estimated with the 36Cl/10Be ratio, https://doi.org/10.5194/egusphere-2025-1780, 2025b.

https://doi.org/10.5194/egusphere-2026-790
Preprint. Discussion started: 30 March 2026

Kipfstuhl, S., Hamann, I., Lambrecht, A., Freitag, J., Faria, S. H., Grigoriev, D., and Azuma, N.: Microstructure mapping: A new method for imaging deformation-induced microstructural features of ice on the grain scale, Journal of Glaciology, 52, 398–406, https://doi.org/10.3189/172756506781828647, 2006.

Larkman, P., Rhodes, R. H., Stoll, N., Barbante, C., and Bohleber, P.: What does the impurity variability at the microscale represent in ice cores? Insights from a conceptual approach, Cryosphere, 19, 1373–1390, https://doi.org/10.5194/tc-19-1373-2025, 2025.

Mulvaney, R., Oates, K., and Wolff, E. W.: Sulphuric acid at grain boundaries in Antarctic ice, Nature, 331, 247–249, https://doi.org/10.1038/331247a0, 1988.

Mulvaney, R., Wolff, E. W., Grieman, M. M., Hoffmann, H. H., Humby, J. D., Nehrbass-Ahles, C., Rhodes, R. H., Rowell, I. F., Parrenin, F., Schmidely, L., Fischer, H., Stocker, T. F., Christl, M., Muscheler, R., Landais, A., and Prié, F.: The ST22 chronology for the Skytrain Ice Rise ice core – Part 2: An age model to the last interglacial and disturbed deep stratigraphy, Climate of the Past, 19, 851–864, https://doi.org/10.5194/cp-19-851-2023, 2023.

Muscheler, R., Beer, J., Kubik, P. W., and Synal, H. A.: Geomagnetic field intensity during the last 60,000 years based on 10Be and 36Cl from the Summit ice cores and 14C, Quaternary Science Reviews, 24, 1849–1860, https://doi.org/10.1016/j.quascirev.2005.01.012, 2005.

Ng, F. S.: Pervasive diffusion of climate signals recorded in ice-vein ionic impurities, Cryosphere, 15, 1787–1810, https://doi.org/10.5194/tc-15-1787-2021, 2021.

Nguyen, L., Paleari, C. I., Müller, S., Christl, M., Mekhaldi, F., Gautschi, P., Mulvaney, R., Rix, J., and Muscheler, R.: The potential for a continuous 10Be record measured on ice chips from a borehole, Results in Geochemistry, 5, 100012, https://doi.org/10.1016/j.ringeo.2021.100012, 2021.

Nguyen, L., Suttie, N., Nilsson, A., and Muscheler, R.: A novel Bayesian approach for disentangling solar and geomagnetic field influences on the radionuclide production rates, Earth, Planets and Space, 74, 1–19, https://doi.org/10.1186/s40623-022-01688-1, 2022.

Nilsson, A., Nguyen, L., Panovska, S., Herbst, K., Zheng, M., Suttie, N., and Muscheler, R.: Holocene solar activity inferred from global and hemispherical cosmic-ray proxy records, Nature Geoscience, 17, 654–659, https://doi.org/10.1038/s41561-024-01467-5, 2024.

Nishiizumi, K., Imamura, M., Caffee, M. W., Southon, J. R., Finkel, R. C., and McAninch, J.: Absolute calibration of 10Be AMS standards, Nuclear Instruments and Methods in Physics Research, Section B: Beam Interactions with Materials and Atoms, 258, 403–413, https://doi.org/10.1016/j.nimb.2007.01.297, 2007.

Raisbeck, G. and Yiou, F.: 10Be in Polar Ice and Atmospheres, Annals of Glaciology, 7, 138–140, https://doi.org/10.3189/s0260305500006054, 1985.

Raisbeck, G. M., Yiou, F., Fruneau, M., Loiseaux, J. M., Lieuvin, M., Ravel, J. C., and Lorius, C.: Cosmogenic 10Be concentrations in Antarctic ice during the past 30,000 years, Nature, 292, 825–826, https://doi.org/10.1038/292825a0, 1981.

Raisbeck, G. M., Yiou, F., Cattani, O., and Jouzel, J.: 10Be evidence for the Matuyama–Brunhes geomagnetic reversal in the EPICA Dome C ice core, Nature, 444, 82–84, https://doi.org/10.1038/nature05266, 2006.

Röthlisberger, R., Mulvaney, R., Wolff, E. W., Hutterli, M. A., Bigler, M., de Angelis, M., Hansson, M. E., Steffensen, J. P., and Udisti, R.: Limited dechlorination of sea-salt aerosols during the last glacial period: Evidence from the European Project for Ice Coring in Antarctica (EPICA) Dome C ice core, Journal of Geophysical Research: Atmospheres, 108, 1–6, https://doi.org/10.1029/2003jd003604, 2003.

Sakurai, T., Ohno, H., Motoyama, H., and Uchida, T.: Micro-droplets containing sulfate in the Dome Fuji deep ice core, Antarctica: findings using micro-Raman spectroscopy, Journal of Raman Spectroscopy, 48, 448–452, https://doi.org/10.1002/jrs.5040, 2017.

Stringer, C., Wang, T., Michaelos, M., and Pachitariu, M.: Cellpose: a generalist algorithm for cellular segmentation, Nature Methods, 18, 100–106, https://doi.org/10.1038/s41592-020-01018-x, 2021.

https://doi.org/10.5194/egusphere-2026-790
Preprint. Discussion started: 30 March 2026

Svensson, A., Bigler, M., Kettner, E., Dahl-Jensen, D., Johnsen, S., Kipfstuhl, S., Nielsen, M., and Steffensen, J. P.: Annual layering in the NGRIP ice core during the Eemian, Climate of the Past, 7, 1427–1437, https://doi.org/10.5194/cp-7-1427-2011, 2011.

Wagner, G.: Die kosmogenen Radionuklide 10Be und 36Cl im Summit-GRIP-Eisbohrkern., Ph.D. thesis, ETH Zürich, 1998.

Wagner, G., Masarik, J., Beer, J., Baumgartner, S., Imboden, D., Kubik, P. W., Synal, H. A., and Suter, M.: Reconstruction of the geomagnetic field between 20 and 60 kyr BP from cosmogenic radionuclides in the GRIP ice core, Nuclear Instruments and Methods in Physics Research, Section B: Beam Interactions with Materials and Atoms, 172, 597–604, https://doi.org/10.1016/S0168-583X(00)00285-8, 2000.

Wedepohl, K. H.: The composition of the continental crust, Geochimica et Cosmochimica Acta, 59, 1217–1232, https://doi.org/10.1016/0016-7037(95)00038-2, 1995.

Willerslev, E., Cappellini, E., Boomsma, W., Nielsen, R., Hebsgaard, M. B., Brand, T. B., Hofreiter, M., Bunce, M., Poinar, H. N., Dahl-Jensen, D., Johnsen, S., Steffensen, J. P., Bennike, O., Schwenninger, J. L., Nathan, R., Armitage, S., Hoog, C. J. D., Alfimov, V., Christl, M., Beer, J., Muscheler, R., Barker, J., Sharp, M., Penkman, K. E., Haile, J., Taberlet, P., Gilbert, M. T. P., Casoli, A., Campani, E., and Collins, M. J.: Ancient biomolecules from deep ice cores reveal a forested southern Greenland, Science, 317, 111–114, https://doi.org/10.1126/science.1141758, 2007.

Zheng, M., Sturevik-Storm, A., Nilsson, A., Adolphi, F., Aldahan, A., Possnert, G., and Muscheler, R.: Geomagnetic dipole moment variations for the last glacial period inferred from cosmogenic radionuclides in Greenland ice cores via disentangling the climate and production signals, Quaternary Science Reviews, 258, https://doi.org/10.1016/j.quascirev.2021.106881, 2021.